




ROLE OF NANOLYCOPENE EMULSION ON THE SUBMANDIBULAR SALIVARY GLANDS OF RATS EXPOSED TO CHRONIC STRESS (HISTOLOGICAL, ULTRASTRUCTURAL AND IMMUNOHISTOCHEMICAL STUDY)

Laila F. Elshahed *, Doaa A. Labah *, Ola M. El-Borady **
and Mervat M. Youssef ***

ABSTRACT

The purpose of this research was to determine the effect of chronic stress on the structure of the rat submandibular salivary gland and the involvement of a nanolycopene emulsion in mitigating this effect. In this research, forty adult male albino rats were divided into four equal groups: group 1 (control group), group 2 (nanolycopene group), group 3 (stress group) and group 4 (stress+ nanolycopene group). The experiment continued for 4 weeks. Serum corticosterone level was assessed at the end of the experiment and submandibular salivary glands were processed for histological, ultrastructural study and immunohistochemical analysis of proliferating cell nuclear antigen. The results showed that rats exposed to chronic stress exhibited significant increase in serum corticosterone level. Histological and ultrastructural examination of their submandibular salivary glands revealed many signs of degeneration with marked intracellular changes in the cytoplasmic and nuclear structure of the acinar and ductal cells. Besides, the glands showed significant reduction in proliferating cell nuclear antigen immunorexpression. Interestingly, intake of nanolycopene emulsion during chronic stress abolished stress elevating effect on serum corticosterone level. The submandibular salivary glands regained its almost normal architecture and the proliferating cell nuclear antigen expression simulated the control group. *Conclusion:* Exposure to chronic stress caused deleterious effects on rats' submandibular salivary glands. However, nanolycopene emulsion was able to ameliorate chronic stress effects. Hence, it is highly recommended to use nanolycopene emulsion daily for individuals subjected to chronic stressful life.

KEYWORDS: Chronic stress, Nanolycopene emulsion, Serum corticosterone level, Submandibular salivary gland.

* Oral Biology Department, Faculty of Dentistry, Zagazig University, Zagazig, Egypt.

** Nanoscience Department, Institute of Nanoscience and Nanotechnology, Kafrelsheikh University, Kafrelsheikh, Egypt.

*** Oral Biology Department, Faculty of Dentistry, Suez Canal University, Ismailia, Egypt.

INTRODUCTION

Lycopene “the naturally occurring carotenoid pigment” has attracted widespread attention in last few years due to its well documented health benefits^[1]. Numerous preclinical and clinical studies have shown that lycopene consumption reduces the risk of chronic illnesses^[2]. These health benefits attributed to antioxidant activity of lycopene which is thought to be due to the unsaturated chemical structure of lycopene that helps its molecule to scavenge singlet oxygen^[3]. Unfortunately, this unsaturated chemical structure plays an important role in its instability, poor solubility, inefficient systemic delivery and low bioavailability^[4].

Nanoencapsulation has been used to tackle these issues due to its enhanced stability, protection from degradation and oxidation during storage period, controlled release to targeted^[5]. Nanoemulsion is a particularly effective delivery system designed for lycopene as it has the advantages of simple preparation, greater safety, long-term stability and easy industrialization^[6].

In modern world, stress is seen as a normal part of life and may be blamed for a wide variety of health problems^[7]. Mild stress may be beneficial, since it has been shown to improve performance on physical and cognitive activities. Chronic, high-intensity stress, on the other hand, results in anxiety and depression^[8].

The activation of stress neuronal circuits is a critical component of the stress response^[9]. The sympathetic adrenomedullary (SAM) and hypothalamic-pituitary-adrenocortical (HPA) axis play a critical role in this process because they act as signaling routes linking the stress center to the rest of the body^[10]. Activation of both systems helps the body to adapt and cope up with the new situations. However, chronic and long lasting stresses induce maladaptation and pathology^[11].

Chronic unpredictable mild stress (CUMS) in rodents is a widely used model of depressive- and anxiety-like behavior with good predictive as well

as constructs validity. The idea of CUMS rely on mixing different types of stressors that the animals cannot predict what will happen next and therefore it is harder to adapt to the situation^[12]. This model has been demonstrated to exhibit depression-related pathophysiological changes that are responsive to antidepressant therapy^[13].

Having nervous and hormonal regulation, it's not surprising to consider the SMG as a good model to study the effect of stress. In addition to its well-known exocrine function through salivary secretion, rodent SMG is believed to exhibit an endocrine function through the presence of granular convoluted tubules (GCT) within the gland secreting biologically active peptides which modify a variety of functions including growth and differentiation, enzymatic control, homeostatic regulation, and adaptation to stress^[14].

Accordingly, this research was conducted to determine the effect of CUMS on the structure of rat SMG and the role of nanolycopene emulsion in mitigating this effect.

MATERIAL AND METHODS

Fabrication of nanolycopene emulsion

Preparation of nanolycopene emulsion from lycopene extract

Lycopene extract was purchased from Puritan's pride premium, Inc. (Holbrook, USA) in the form of rapid release soft gel capsules each one contain 40mg lycopene. Poly lactic-co-glycolic acid (PLGA) (Purac Biomaterials, Holland) was used as a carrier system. The PLGA encapsulated lycopene were prepared using solid/oil/water, an emulsification-solvent evaporation/diffusion process with slight modification^[15].

The characterization techniques of nanolycopene emulsion

The size and form of the generated nanoemulsion were determined using transmission electron

microscopy using a JEOL microscope (Model type JEM-2010) operated at a 200 kV accelerating voltage and connected to a Gatan camera (Model type Erlangshen ES500). The structural information was obtained using an FTIR analysis with a wavelength range of 4000 to 400 cm⁻¹ on a JASCO-Spectrometer; the measurement was performed on liquid NPs. At 25°C, zeta-potential measurements were made in a disposable cell using a Zetasizer Nano ZS (Model type, Malvern).

Experimental design

This study was conducted after the approval of ethical committee at Faculty of Dentistry, Suez Canal University (number: 321/2012). Sample size estimation was calculated according to a previous study Charan et al. [16] with a total of 40 samples classified into four equal groups (10 in each).

Animal grouping

Forty adult male albino rats weighing an average of 150-180 grams were used in this study. They were kept in rat cages, numbered, named, and maintained at Faculty of Medicine, Zagazig University in a well-ventilated animal house. The room temperature and humidity were maintained at 23°C and 60%, respectively, while maintaining a typical photoperiod. Dry rat pellets were fed to the rats, and they were allowed unrestricted access to water. After one week acclimatization period, the animals were randomly allocated into 4 equal groups: Group 1 (control group) was served as a negative control for the experimental groups. Group 2 (nanolycopene group) was received 6 mg/kg b.w/day of nanolycopene emulsion by oro-gastric intubations for 4 weeks [17]. Group 3 (stress group) was exposed to CUMS for 4 weeks (Table 1) [18]. Group 4 (stress+nanolycopene group) was exposed to CUMS similar to group 3 and received nanolycopene emulsion similar to group 2 for 4 weeks.

Analysis of plasma corticosterone

Serum corticosterone (SCC) level was measured at research unit of Clinical Pathology Department,

Zagazig University Hospital. After rat anesthesia, blood sample were taken early in the morning at the end of the experimental period from rats' retro orbital sinus collected in plain tubes and was allowed to clot at 37°C for 30 minutes then centrifuged at 3000 rpm for 5 minutes. The clear supernatant sera were separated from the clot and were used for quantitative measurement of SCC using solid phase enzyme linked immunosorbent assay (ELISA) [19].

Rat euthanasia

At the end of the experiment and following the collection of blood samples, all rats were euthanized with an overdose of sodium thiopental (EIPICO, Egypt) followed by cervical dislocation. Each animal's SMGs were thoroughly dissected. The right glands were processed for histological and immunohistochemical analysis, whilst the left glands were prepared for electron microscopic analysis.

Histological examination

For 48 hours, specimens from the right SMGs were kept in 10% buffered formalin solution. After fixation, the specimens were dehydrated in increasing concentrations of ethyl alcohol, washed with xylene, and embedded in paraffin. Each block was sectioned using a microtome, and five serial slices (5m thick) were produced and stained with hematoxylin and eosin (H&E) to assess any structural abnormalities in SMGs histologically. The slides were analyzed and shot using a digital color CCD camera (Olympus, DP73, Tokyo, Japan) mounted on a light microscope (Olympus BX53, Tokyo, Japan) at X400 magnification in Faculty of Medicine, Zagazig University.

Immunohistochemical analysis

PCNA expression was used as a well-known marker for cell proliferation to detect any possible changes in its index [20]. Immunohistochemistry was used to identify PCNA expression using the Avidin–Biotin–Complex (ABC) approach. The presence of

TABLE (1): List of stressors used for CUMS induction

	Day 1	Day 2	Day 3	Day 4	Day 5	Day 6	Day 7
Week 1	Restraint stress	Placement in an empty cage with water at the bottom + lights on	Tilt cage at 30 degrees	Placement in cages with wet sawdust	Placement in soiled cages of other rats	Restraint stress	Reversal of the light dark cycle /
	(4 hours)	(4 hours)	(4 hours)	(4 hours)	(4 hours)	(4 hours)	-
Week 2	Placement in an empty cage with water at the bottom + lights on	Tilt cage at 30 degrees	Placement in cages with wet sawdust	Placement in soiled cages of other rats	Restraint stress	Placement in an empty cage with water at the bottom + lights on	Reversal of the light dark cycle/
	(4 hours)	(4 hours)	(4 hours)	(4 hours)	(4 hours)	(4 hours)	-
Week 3	Tilt cage at 30 degrees	Placement in cages with wet sawdust	Placement in soiled cages of other rats	Restraint stress	Placement in an empty cage with water at the bottom + lights on	Tilt cage at 30 degrees	Reversal of the light dark cycle/
	(4 hours)	(4 hours)	(4 hours)	(4 hours)	(4 hours)	(4 hours)	-
Week 4	Placement in cages with wet sawdust	Placement in soiled cages of other rats	Restraint stress	Placement in an empty cage with water at the bottom + lights on	Tilt cage at 30 degrees	Placement in cages with wet sawdust	Reversal of the light dark cycle/
	(4 hours)	(4 hours)	(4 hours)	(4 hours)	(4 hours)	(4 hours)	-

a brown-colored reaction restricted to the nucleus was characterized as a positive PCNA response. Two experienced research colleagues determined the number of positive immunoreactions utilizing blinded analysis through light microscope (Olympus BX53, Tokyo, Japan) at X400 magnification and image analysis using the Image J software (version 4.10.03, Nikon, Tokyo, Japan).

Transmission electron microscopic examination

The left SMGs were cut into 1 mm cubes and fixed in a solution of 4% paraformaldehyde and 1% glutaraldehyde for 2 hours at room temperature. Following that, they were rinsed and postfixed with 1% osmium tetroxide. After fixation, the samples were dried in a stepwise ethanol series, submerged in 100% actone, and embedded in epon. Ultrathin

slices were cut on an RMC-USA ultramicrotome, picked on copper grids, stained with uranyl acetate and lead citrate, and analyzed at the Electron Microscopy Unit at Mansoura University using a JEOL JEM-2100 transmission electron microscope (Jeol Ltd, Tokyo, Japan).

Statistical analysis

Data were collected from SCC analysis and PCNA immunohistochemical analysis then were tabulated and statistically analyzed by statistical package for social sciences (SPSS) software using one-way analysis of variance (ANOVA) followed by post hoc test to reveal statistical difference among groups. Results were considered statistically significant at $P < 0.05$.

RESULTS

Morphological and structural characteristics of the developed nanolycopene

Morphological analysis

Analysis of the size and shape of the developed nanoparticles (PLGA encapsulated lycopene) was detected by transmission electron microscope revealed homogenous and perfectly spherical shaped particles. The size of developed particles was around 190 nm (Fig. 1 A). The particles are separated from each other without aggregation which indicates the effectiveness of capping and stabilizing agent used.

The FTIR spectroscopy

The interaction between lycopene and the other added materials during nano-emulsion preparation was detected by noticing the functional groups present in the emulsion using the FTIR spectroscopic analysis (Fig. 1 B). The broad band appeared at 3362.19 cm^{-1} , corresponding to O-H stretching vibration present in the PLGA. The vibration band of lycopene C-H stretch appeared at 2840 cm^{-1} . Furthermore the scissoring vibration of CH_2 located at 1418 cm^{-1} and the CH_3 deformation peak appeared at 1375 cm^{-1} , the $\text{R}_2\text{C}=\text{CR}$ was noticed at 511 cm^{-1} , stretching vibration of $\text{C}=\text{C}$ at 1550 cm^{-1} , C-O symmetric stretch present in the PLGA emerged at 1646.85 cm^{-1} . Stretching band of C-C at 1155 cm^{-1} . The presence of functional groups like C=O, C-O, and O-H suggests the linkage of the PLGA to lycopene.

The Zeta potential analysis

The Zeta potential measurement is considered as an indication for the colloidal stability as well as the particles surface charges. The zeta potential detected for the synthesized nanolycopene was -17.1 mV (Fig. 1 C). This highly negative zeta potential value reflects that nano emulsion possesses an

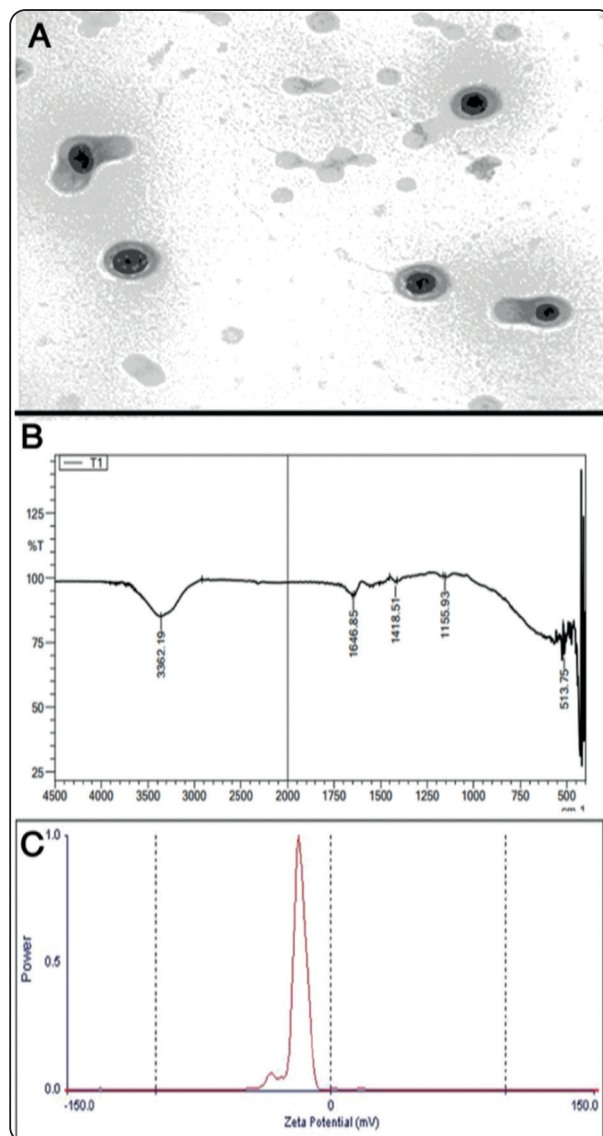


Fig. (1) Photographs show morphological and structural characterization of nanolycopene. A. Electron micrograph of the developed nanolycopene. (Orig. Mag X 15000). B. The FTIR spectrum of the nanolycopene. C. The zeta potential of nanolycopene.

efficient stabilization and high stability. The present nanoemulsion showed high stability compared to the nanolycopene prepared using polyethylene glycol and tween 80 that exhibited nanolycopene with $+4.79\text{ mV}$.

Serum corticosterone results

Analysis of the mean SCC level revealed that nanolycopene group showed no significant

difference than the control group. However, stress group showed marked significant increase above the control group. On the other hand, nanolycopene + stress group exhibited significant decrease below that of stress group but persisted significant increase above the control group (Table 2).

TABLE (2): The mean and standard deviation of SCC among the four different groups.

Groups	Mean	SD	F	P value 0.05
Group 1 (Control)	216.66 ^c	7.04	35.19	0.00**
Group 2 (Nanolycopene)	223.05 ^c	3.59		
Group 3 (Stress)	734.16 ^a	3.70		
Group 4 (Nanolycopene + stress)	536.94 ^b	6.59		

** , a, b: means significant differences between groups at $P < 0.05$

Histological results

Control group showed the architecture of a normal SMG. It consisted of serous acini acini, various types of ducts and connective tissue stroma. The serous acini were numerous, rounded, small in size and had narrow lumens. They were composed of roughly pyramidal cells with basophilic cytoplasm and large, prominent, spherical basally located nuclei. The intercalated ducts were compressed between the acini. They appeared small and lined with cuboidal cells with centrally located nuclei and little cytoplasm. The GCTs appeared large in size, mostly rounded and lined with columnar cells with large rounded basally situated nuclei together with large numbers of apical eosinophilic granules. The striated ducts were lined with simple columnar cells characterized by their basal striations, centrally placed rounded nuclei and intensely stained eosinophilic cytoplasm. In addition, blood

capillaries were detected adjacent to the intralobular ducts and in the connective tissue septa (Fig. 2 A). Examination of the SMG in nanolycopene group revealed resemblance to that of control group (Fig. 2 B). However, stress group revealed altered gland architecture. Some acinar cells revealed destruction and loss of cytoplasm leaving vacuoles along with diversity in their nuclear size, shape and number. Many signs of degeneration were noted in the ducts where cells had abnormal outlines and abnormal nuclear shape. Some ductal cells exhibited vacuolization and destruction of cytoplasm. The blood capillaries appeared congested and dilated (Fig. 2 C). Interestingly, stress + nanolycopene group showed marked improvement in their acinar and ductal cells compared to stress group. However, little areas of separation between acini were noticeable and some acinar cells appeared binucleated (Fig. 2 D).

Immunohistochemical results:

Examination of PCNA immunohistochemical expression revealed strong nuclear staining of acinar and ductal cells with anti- PCNA antibody in control and nanolycopene groups. On the other hand, stress group exhibited weak nuclear staining of acinar and ductal cells. Whereas nanolycopene + stress group showed improved PCNA immunoreactivity than stress group and depicted moderate to strong nuclear staining of acinar and ductal cells (Fig. 3 A-D).

Statistical analysis of the number of positively immunostained cells for PCNA demonstrated that control group simulated those of nanolycopene and nanolycopene + stress groups with no significant difference between them regarding the number of their positive PCNA immunostained cells. Conversely, stress group revealed a significant decrease in the number of PCNA positively immunostained cells in comparison with those of other groups namely; control, nanolycopene and nanolycopene + stress groups (Fig 4 & Table 3).

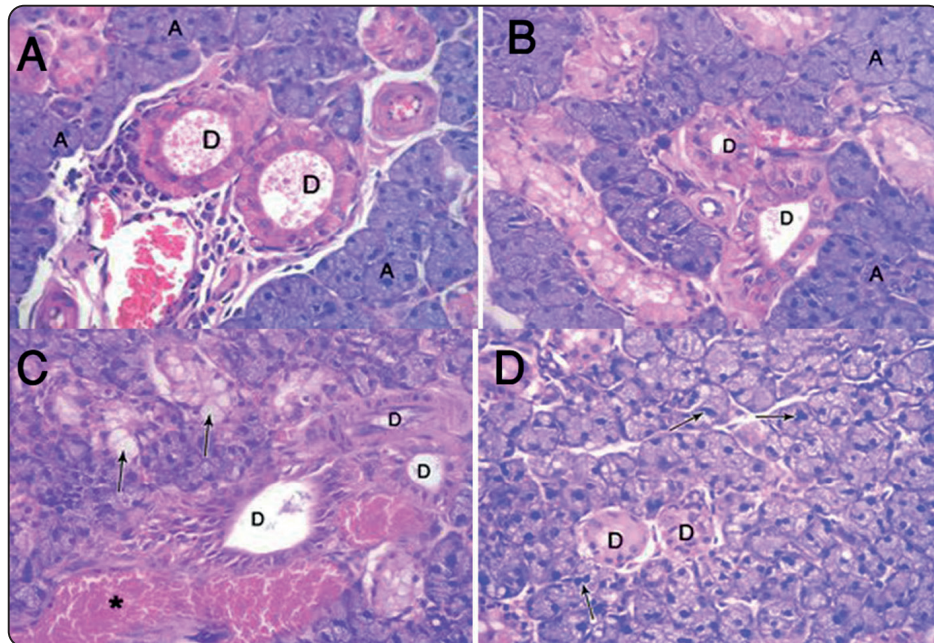


Fig. (2). Light photomicrographs of the SMG stained with H& E stain. A. shows the SMG of the control group with normal histological structure; serous acini (A), striated ducts (D). B. shows the SMG of the nanolycopene emulsion group with normal histological structure resembling the control group. C. shows an altered gland architecture in stress group with vacuolization of the cells (arrows), many congested and dilated blood capillaries (*), and ducts depict abnormal cells configuration (D). D. shows marked improvement in the SMG of the stress + nanolycopene group however some cells appeared binucleated (arrows). (H& E, A-D X 400)

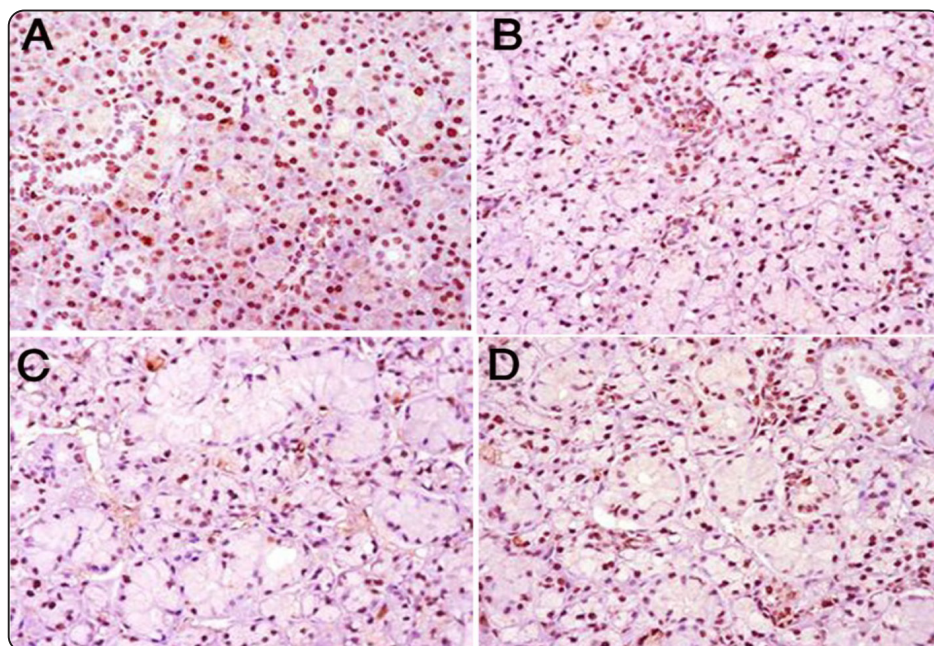


Fig. (3). Photomicrographs of PCNA immunohistochemical-stained sections of the SMGs of different groups. A. control group shows strongly positive staining. B. nanolycopene emulsion group shows also strong reactivity. C. stress group shows weak positive staining reaction. D. nanolycopene emulsion + stress group shows moderate to strong positive staining. (PCNA immunostain, A-D X 400).

TABLE (3): The mean and standard deviation of PCNA expression among groups.

Groups	Mean	SD	F	P value
Group 1 (Control)	216.09 ^a	3.231	31.87	0.00**
Group 2 (Nanolycopene)	215.548 ^a	2.759		
Group 3 (Stress)	161.628 ^b	4.418		
Group 4 (Nanolycopene + stress)	213.174 ^a	2.811		

***, a, b: means significant differences between groups at P < 0.05*

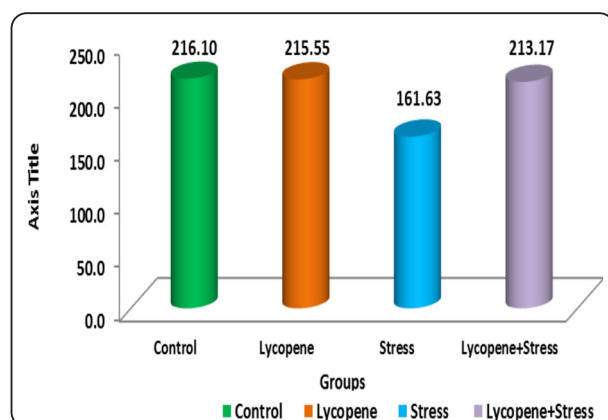


Fig. (4). Bar chart shows the mean of PCNA expression among the four groups.

Transmission electron microscopic results

The SMG of control group revealed normal ultrastructure findings. The acinar portion formed from pyramidal cells with basally situated nuclei. The well-developed parallel arrays of RER occupied mainly the basal part of the cell. The intercalated duct depicted central lumen encircled by cuboidal cells with rounded euchromatic nuclei and few mitochondria. The GCT was lined with columnar cells with rounded euchromatic nuclei and large number of apical electron dense granules. The striated duct was lined with simple columnar epithelium with rounded euchromatic nuclei and basal infolding of cell membrane alternating with abundant vertically arranged mitochondria (Fig. 5 A-D). The SMG of nanolycopene group displayed ultrastructure resemblance to control group (Fig. 5 E-H). Conversely, the SMG of stress group revealed several degenerative changes. The acinar cells depicted abnormal shape of secretory granules, dilated RER and some nuclei had destructed chromatin. The intercalated duct cells revealed cytoplasmic vacuolization and abnormally shaped nuclei with disturbed chromatin pattern and irregular nuclear membrane. The GCT cells appeared binucleated with highly condensed chromatin and the cytoplasm showed swollen mitochondria and diffusely dispersed RER. The striated duct cells showed cytoplasmic rarefaction and dispersed RER. Mitochondria exhibited swelling, ballooning and rupture (Fig. 5 I-L). Electron microscopic examinations of the SMG of nanolycopene + stress group revealed improvements in acini and ducts compared to stress group (Fig. 5 M-O).

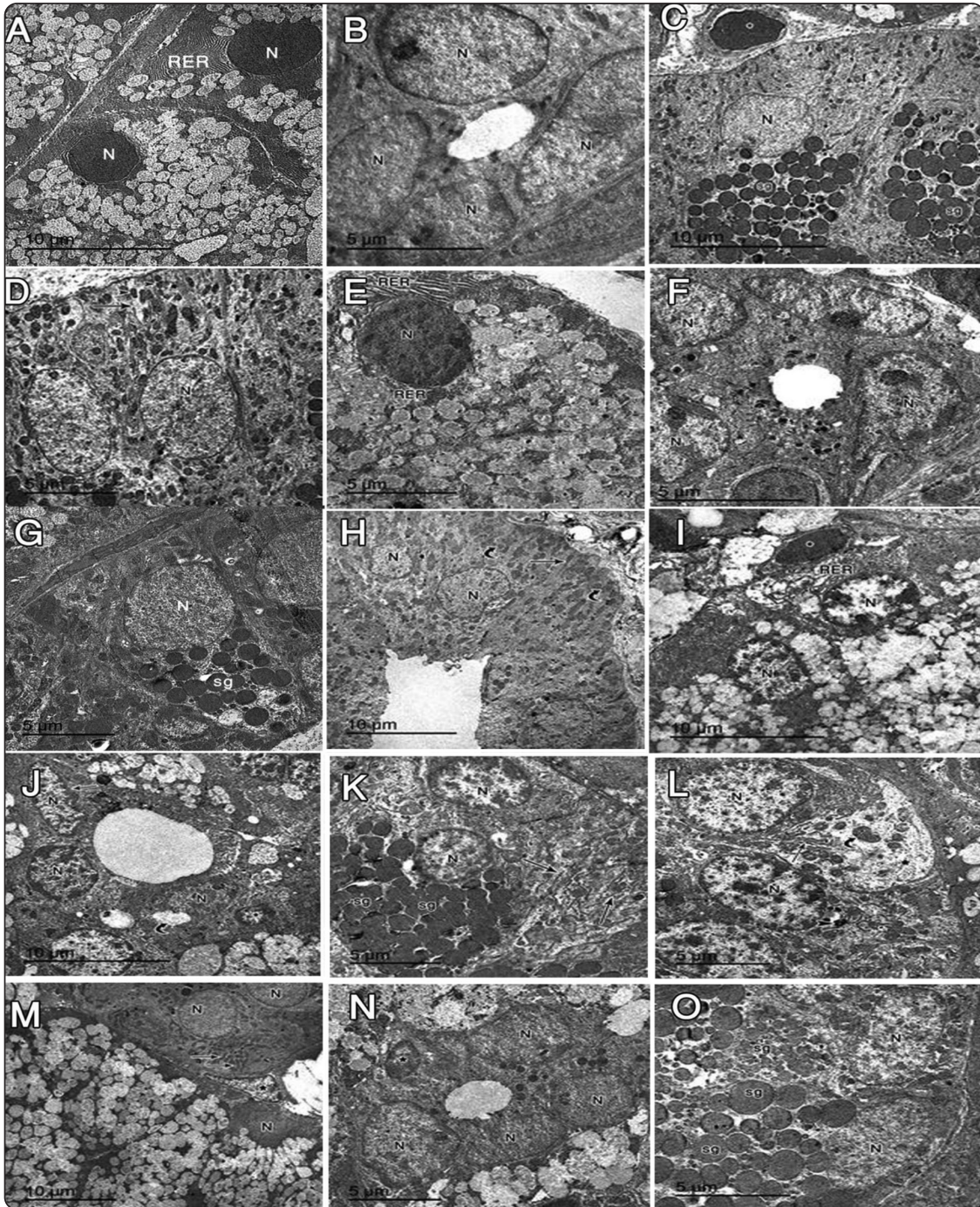


Fig. (5). Electron micrograph of the SMGs of different groups. The SMG of control group shows normal shape; A. acinar cells, B. intercalated duct, C. GCT and D. striated duct. The SMG of nanolycopene group displays resemblance to control group; E. acinar cells, F. intercalated duct, G. GCT and H. striated duct. The SMG of stress group reveals degenerative changes; I. acinar cells with abnormal shape of secretory granules, dilated RER and some nuclei had destructed chromatin, J. intercalated duct with cytoplasmic vacuoles (curved arrow) and abnormally shaped nuclei with disturbed chromatin, K. GCT with swollen mitochondria and diffusely dispersed RER (arrows). L. striated duct shows swollen mitochondria (curved arrow), diffusely dispersed RER (arrow) and rarefaction of cytoplasm (*). The SMG of nanolycopene + stress group reveals improvements; M. almost normal acinar cells and striated duct regains its characteristic basal striation (arrows), N. improved intercalated duct however highly condensed pyknotic nucleus could be noted (*), O. almost normal GCT. nucleus (N), secretory granules (SG) and rough endoplasmic reticulum (RER).

DISCUSSION

The present study attempted to address two research points. The first, the possible degenerative effects of chronic stress on the rat SMGs. The second, the proficiency of nanolycopene emulsion as an emerging nano- nutraceutical to alleviate those effects.

To accomplish the current work, adult male rats were the experimental model of choice since they were successfully adopted experimental model in the previous CUMS researches that has enriched to clinical models of anxiety and depression^[12]. Also, rats were successfully contributed at large towards the development of drugs used in the treatment of psychological and psychiatric disorders that are common among the human beings in the modern century^[21].

In the present study, rats of stress group exhibited significant increase of their SCC above the control level. This result verified the effectiveness of CUMS protocol used in the current study in inducing stress and activating the HPA axis. Moreover, this finding was in agreement with Liu et al. who depicted marked increased SCC in animals exposed to CUMS^[22]. Similarly, Lee et al. reported elevated serum level of cortisol in association with chronic stress and depressive disorders in human and they proved the potential of utilizing cortisol as a biomarker for chronic stress and depressive disorders^[23]. The increased SCC might be explained by the concept that stressful events overcome the normal negative feedback control of cortisol by circulating glucocorticoids, which operate on the hypothalamus to prevent increased CRF release and, ultimately, ACTH production from the pituitary gland. When there is no perceived stressful event, this negative feedback loop suppresses HPA activity^[24].

Noteworthy in this study, both histological and transmission electron microscopic results depicted loss of normal gland architecture as well as marked intracellular changes in the cytoplasmic and nuclear structure of the SMG cells of the stressed-rat.

Therefore, it is imperative to recall that psychological stress was reported to be converted into cellular stress response ranging from the activation of survival pathways to the initiation of cell death depending to a large extent on the nature and duration of the stress^[25, 26]. Additionally, psychological stress has been associated with oxidative stress, which occurs when there is an imbalance between the creation of reactive oxygen species (ROS) by cells and their antioxidant defence mechanisms. This is reasonable given the established link between psychological stress and increased oxidant production and high levels of oxidative damage, and hence the likelihood that prolonged exposure to psychological stressors may raise the risk of acquiring a range of diseases^[27, 28].

In accordance with the depicted histological and ultrastructural destructive changes, the SMG of stressed- rats exhibited significant decrease in the number of PCNA positively immunostained cells in comparison with those of control group. This finding could be attributed to the degenerative changes and apoptosis caused by CUMS on the SMG cells. Similar result was reported by Tian et al. who observed that PCNA expression was significantly decreased in the testis of rats exposed to chronic stress^[29]. Rentscher et al. previously established that chronic stress exposure and daily stressful experiences induce cellular senescence, a stable state of cell cycle arrest, and they provided evidence for the hypothesis that chronic stress accelerates ageing by inducing cellular senescence, which is a frequent correlate of age-related diseases^[30].

Surprisingly in the present work, rats received a daily dose of nanolycopene emulsion and exposed to CUMS for 4 weeks revealed significant decrease in their SCC below that of stress group denoting potential recovery from stress-induced changes. The current decline in SCC was in accordance with that of Paruchuri et al. who reported that lycopene intake in rats exposed to CUMS exhibited a significant

decrease in their SCC levels below that of rats exposed only to CUMS^[31].

Similarly, both histological and ultrastructural examination revealed that the SMG regained its almost normal architecture along with marked enhancement in cellular shape and component of the acini and ducts. The beneficial role of nanolycopene emulsion in improving CUMS-altered SMGs matched that of Kumar et al. who evaluated the effects of lycopene on CUMS-induced depressive-like behavioral changes in rats and stated that lycopene possessed antidepressant activity which may be due to its antioxidant effect [32]. Noteworthy, Paruchuri et al. reported that lycopene supplementation in rats exposed to CUMS significantly reversed the oxidative stress by increasing the antioxidant enzymes activity including; superoxide dismutase, catalase and glutathione peroxidase enzymes thereby raising the efficiency of antioxidant defense system^[31]. Additionally, previous research has shown that lycopene is the most powerful antioxidant and a potent scavenger of free radicals^[33]. It inhibits lipoperoxidation and has a direct effect on a variety of molecular signaling pathways involved in the activation of the antioxidant defense system, including mitogen-activated protein kinases (MAPK), ROS-generating enzymes, and nuclear factor- κ B (NF- κ B)^[34].

However, stressed- rats received nanolycopene emulsion revealed minor microscopic changes in the SMG concomitant with persistent increase in SCC above the normal level. These findings suggested that consumption of nanolycopene emulsion needs a longer period to reach the absolute recovery of stress-induced changes.

More interestingly in this study, the number of PCNA positively immunostained cells in the SMG of stressed- rats received nanolycopene emulsion simulated that of control group and displayed significant increase in comparison with those of stress group. These findings could be explained by

Astley et al. who verified that lycopene is capable of exerting antioxidant protection by scavenging DNA-damaging free radicals and enhancement of DNA repair^[35]. Moreover, Scovassi et al. demonstrated elevated PCNA expression in cells under DNA repair and illustrated that PCNA can participate in different pathways of DNA repair^[36].

Lycopene was used in the current study in the form of a nanolycopene emulsion, since it is crucial to evoke that lycopene's bioaccessibility was greatly boosted in the nanoemulsion system^[37]. Additionally, lycopene nanoemulsions with droplet sizes of 100–200 nm exhibited remarkable anti-radical and antioxidant action^[38].

CONCLUSION

Chronic stress has adverse effects that could induce pathological changes in the rat SMG. However, nanolycopene emulsion displayed a prospective role in the protection of SMG from stress-induced changes.

Recommendation

Further studies are recommended to prove the capability of nanolycopene emulsion to treat stress hazards on different body tissues and whether its beneficial role will differ among different ages and gender. Also, it is highly recommended to investigate the capability of nanolycopene emulsion to treat salivary gland destruction of other origins.

REFERENCES

1. Adetunji CO, Akram M, Mtewa AG, Jeevanandam J, Egbuna C, Ogodo AC, et al. Biochemical and pharmacoh therapeutic potentials of lycopene in drug discovery. In: Preparation of Phytopharmaceuticals for the Management of Disorders. The Development of Nutraceuticals and Traditional Medicine. Elsevier, Amsterdam, Netherlands. 2021; pp. 307-360.
2. Kim JH, Lee J, Choi IJ, Kim YI, Kwon O, Kim H, et al. Dietary carotenoids intake and the risk of gastric cancer: A case control study in Korea. *Nutrients*. 2018; 10: 1031-1050.

3. Stajčić S, Četković G, Čanadanović-Brunet J, Djilas S, Mandić A, Četojević-Simin D. Tomato waste: Carotenoids content, antioxidant and cell growth activities. *Food Chem.* 2015; 172: 225-232.
4. Liang X, Ma C, Yan X, Liu X, Liu F. Advances in research on bioactivity, metabolism, stability and delivery systems of lycopene. *Trends Food Sci. Tech.* 2019; 93: 185-196.
5. Rehman A, Tong Q, Jafari SM, Assadpour E, Shehzad Q, Aadil RM, et al. Carotenoid-loaded nanocarriers: A comprehensive review. *Adv. Colloid Interfac. Sci.* 2019; 275; 102048.
6. Zardini A, Mohebbi M, Farhoosh R, Bolurian S. Production and characterization of nanostructured lipid carriers and solid lipid nanoparticles containing lycopene for food fortification. *J. Food Sci. Technol.* 2018; 55: 287- 298.
7. Slavich GM. Life stress and health: A review of conceptual issues and recent findings. *Teach. Psychol.* 2016; 43: 346-355.
8. Fink G. Stress: concepts, definition and history. In: Reference Module, in *Neuroscience and Biobehavioral Psychology*, Elsevier, Amsterdam, Netherlands. 2017; pp. 1-9.
9. Yiallouris A, Tsioutis C, Agapidaki E, Zafeiri M, Agouridis AP, Ntourakis D, et al. Adrenal aging and its implications on stress responsiveness in humans. *Front Endocrinol.* 2019; 7:10- 54.
10. Dennis S, Charney MD. Psychobiological mechanism of resilience and vulnerability: Implications for successful adaptation to extreme stress. *Am J Psychiatry.* 2004; 161:195- 216.
11. Radley J, Morilak D, Viau V, Campeau S. Maladaptive changes and implications for stress-related CNS disorders. *Neurosci Biobehav Rev.* 2015; 58: 79-91.
12. Koprđova R, Bogi E, Belovičova K, Sedlačkova N, Okuliarova M, Ujházy E, et al. Chronic unpredictable mild stress paradigm in male Wistar rats: effect on anxiety- and depressive-like behavior. *Neuroendocrinol Lett.* 2016; 37:103-110.
13. Kuipers SD, Trentani A, vander Zee EA, denBoer JA. Chronic stress- induced changes in the rat brain: role of sex differences and effects of long- term tianeptine treatment. *Neuropharmacology.* 2013; 75: 426-436.
14. Rougeot C, Rosinski-Chupin I, Mathison R, Rougeon F. Rodent submandibular gland peptide hormones and other biologically activepeptides. *Peptides.* 2000; 21: 443-557.
15. Kim SO, Ha TVA, Choi YJ, Ko SH. Optimization of homogenization–evaporation process for lycopene nanoemulsion production and its beverage applications. *J. Food Sci.* 2014; 79: 1604-1610.
16. Charan J, Biswas T. How to calculate sample size for different study designs in medical research? *Indian J Psychol Med.* 2013; 35:121-126.
17. Stojiljkovic N, Ilic S, Jakovljevic V, Stojanovic N, Stojnev S, Kocic H, et al. The encapsulation of lycopene in nanoliposomes enhances its protective potential in Methotrexate-induced kidney injury model. *Oxid Med Cell Longev.* 2018; 2018: 2627917.
18. Doron R, Lotan D, Versano Z, Benatav L, Franko M, Armoza S. Escitalopram or novel herbal mixture treatments during or following exposure to stress reduce anxiety-like behavior through corticosterone and BDNF modifications. *PLoS One.* 2014; 9: 91455-91464.
19. Kinn Rød AM, Harkestad N, Jellestad FK, Murison R. Comparison of commercial ELISA assays for quantification of corticosterone in serum. *Sci Rep.* 2017; 7(1):6748.
20. Strzalka W, Ziemienowicz A. Proliferating cell nuclear antigen (PCNA): A key factor in DNA replication and cell cycle regulation. *Ann. Bot.* 2011; 107: 1127-1140.
21. D'Souza UJ, Rahaman MS. Stress, psychological, somatic, isolation, restraint, rodent. *MSP.* 2018; 2: 3-5.
22. Liu D, Xie K, Yang X, Gu J, Ge L, Wang X, et al. Resveratrol reverses the effects of chronic unpredictable mild stress on behavior, serum corticosterone levels and BDNF expression in rats. *Behav Brain Res.* 2014; 264: 9-16.
23. Lee DY, Kim E, Choi MH. Technical and clinical aspects of cortisol as a biochemical marker of chronic stress. *BMB Rep.* 2015; 48: 209-216.
24. McEwen BS. Stress, adaptation, and disease: Allostasis and allostatic load. *Ann. N. Y. Acad. Sci.* 1998; 840:33-44.
25. Hayashi T. Psychological stress and cellular stress. *Psychiatry Clin Neurosci.* 2015; 69: 179-191.
26. Fulda S, Gorman AM, Hori O, Samali A. Cellular stress responses: Cell survival and cell death. *Int. J. Cell Biol.* 2010; 2010: 1-23.
27. Salim S. Oxidative stress and psychological disorders. *Curr Neuropharmacol.* 2014; 12: 140-147.

28. Kelly GS. Nutritional and botanical interventions to assist with the adaptation to stress. *Altern Med Rev.* 1999; 4: 249-265.
29. Tian P, Lv P, Shi W, Zhu M, Cong B, Wen B. Chronic stress reduces spermatogenic cell proliferation in rat testis. *Int J Clin Exp Pathol.* 2019; 12: 1921-1931.
30. Rentscher KE, Carroll JE, Repetti RL, Cole SW, Reynolds BM, Robles TF. Chronic stress exposure and daily stress appraisals relate to biological aging marker p16INK4a. *Psychoneuroendocrinology.* 2019; 102: 139-148.
31. Paruchuri K, Naveen V. Effect of lycopene on antioxidant status and serum corticosterone in Wistar rats subjected to chronic mild stress. *J Clin Diagn Res.* 2019; 13: 1-4.
32. Kumar PV, Elango P, Asmathulla S, Kavimani S. Lycopene treatment transposed antidepressant like action in rats provoked to chronic mild stress. *Biomed Pharmacol J.* 2019; 12: 981-988.
33. Omoni AO, Aluko RE. The anti-carcinogenic and anti-atherogenic effects of lycopene: A review. *Trends Food Sci Technol.* 2005; 16: 344-350.
34. Palozza P, Catalano A, Simoner R, Cittadini A. Lycopene as a guardian of redox signaling. *Acta Biochim Pol.* 2012; 59: 21-25.
35. Astley SB, Elliott RM. How strong is the evidence that lycopene supplementation can modify biomarkers of oxidative damage and DNA repair in human lymphocytes? *J Nutr.* 2005; 135: 2071-2073.
36. Scovassi AI, Prosperi E. Analysis of proliferating cell nuclear antigen (PCNA) associated with DNA. *Methods Mol Biol.* 2006; 314: 457-475.
37. Zhao C, Wei L, Yin B, Liu F, Li J, Liu X, et al. Encapsulation of lycopene within oil-in-water nanoemulsions using lactoferrin: Impact of carrier oils on physicochemical stability and bioaccessibility. *Int. J. Biol. Macromol.* 2020; 153: 912-920.
38. Ha TV, Kim S, Choi Y, Kwak HS, Lee SJ, Wen J, et al. Antioxidant activity and bioaccessibility of size-different nanoemulsions for lycopene-enriched tomato extract. *Food Chem.* 2015; 178:115-121.